Normal and superconducting properties of Cs_xWO_3

M. R. Skokan,* W. G. Moulton, and R. C. Morris
Department of Physics, Florida State University, Tallahassee, Florida 32306
(Received 11 May 1979)

The resistivity, Seebeck coefficient, superconducting transition temperature, and upper critical field have been measured in Cs_xWO_3 for $0.19 \leq x \leq 0.30$. In contrast to Rb_xWO_3, no temperature-dependent anomalies were observed in either the normal resistivity or the Seebeck coefficient. The superconducting transition temperature, T_c, increases monotonically with decreasing x from 2 K at $x=0.30$ up to 6.7 K at $x=0.20$, with an inflection near 0.24. The resistivity as a function of x increases monotonically with decreasing x and also has an inflection near $x=0.24$.

I. INTRODUCTION

The properties of the tungsten bronzes, compounds of the composition M_xWO_3 where M is any one of about 40 metallic elements, have been the subject of many previous investigations.[1] These compounds exist in several structural phases, with most of the previous work having concentrated on the cubic phase and particularly on the sodium-tungsten bronzes. However, the hexagonal structure has been shown to be more conducive to superconductivity than the other structures.[1] The hexagonal crystal structure in the plane perpendicular to the c axis is shown in Fig. 1. The x values for this structure are limited to the range $x=0.33$, where all the hexagonal channels are filled, down to the stability limit of the phase $x=0.16$–0.20. Recently,[2] the hexagonal tungsten bronze Rb_xWO_3 has been shown to have a very unusual variation of superconducting and normal properties as a function of the composition (x value). In these compounds the superconducting transition temperature rises with decreasing x from 2 K at $x=0.33$ and then drops below 0.6 K at $x=0.25$ before again rising to above 4 K as x is further decreased to $x=0.16$. This behavior suggests some type of phase boundary may exist near $x=0.25$, although x-ray diffraction studies at several temperatures have shown no evidence of a structural change with composition. Furthermore, temperature-dependent anomalies in the resistivity, Hall coefficient, and Seebeck coefficients were observed at all x values except $x=0.33$. The temperature at which these anomalies occur is dependent on x with the maximum temperature of the anomalous behavior occurring at $x=0.25$—again suggestive of some type of phase boundary at this concentration. These anomalies in the normal electrical properties in themselves appear to result from some type of temperature-dependent phase change. In addition, a large 60° anisotropy in H_{c2} in the plane perpendicular to the c axis is observed for all concentrations, as well as a 180° anisotropy in the plane of the c axis.

Analysis of the normal and superconducting transport behavior observed in Rb_xWO_3 would seem to make it highly unlikely that the anomalous properties are predominantly due to shifts in the Fermi level with x, but that phonon effects and the phonon-electron interaction must play a significant role. These unusual properties in the Rb_xWO_3 system suggested that a careful comparative study of the hexagonal Cs_xWO_3 system might provide further insight into the properties of the hexagonal tungsten bronzes. The conduction mechanism in both systems is the same,[3] i.e., the metal ion donates its electon to the t_{2g} tungsten d band, and one would not expect to first order significant differences in the Fermi surface or density of states between the Rb and Cs tungsten bronzes. Thus the primary differences in the conduction and superconducting properties should be due to differences in the ion sizes relative to the size of the "holes" in the channels and in the mass of the ions, both of which should predominantly affect the phonon spectrum.

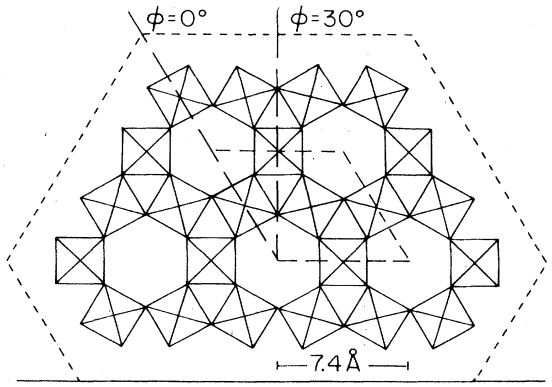

FIG. 1. Diagram of the hexagonal M_xWO_3 lattice structure, after Magneli (Ref. 3). The M ions lie in sites along the open hexagonal channels, which are formed by corner-linked WO_6 octahedra. The structure is filled at $x=0.33$.

II. EXPERIMENTAL METHODS

Single crystals of Cs_xWO_3 were prepared by a thermal vapor growth process, very similar to the methods used in our previous work on Rb_xWO_3.[2] Finely ground reagents of WO_3 (cerac/pure 99.9%−325 mesh), W (alfa inorganic 99.9+%−100 mesh), and Cs_2WO_4 (roc/ric 99.9% anhydrous Cs_2WO_4) were mixed in appropriate amounts for the x value desired and 5 g of the mixture placed in 10 cm long by 1.5 cm diameter quartz tubes. The quartz tubes had previously been washed with HF, rinsed in distilled and deionized water, and heated overnight at 1100 °C under a vacuum of 10^{-6} Torr. The loaded tubes were evacuated to 10^{-6} Torr and held at 400 °C for periods varying from 4 to 16 hours. They were then sealed and heated at 800 °C for 24 hours, raised to 950 °C for 5 to 7 days, and then allowed to cool to room temperature over a 24 hour period. The low x values ($x \approx 0.2$) were the most difficult to grow, and grew as hexagonal needles approximately 20 μm wide and 5 mm long. The intermediate concentrations often grew as platelets as well as hexagonal needles, while the high x values grew exclusively as hexagonal needles. Laue diffraction confirmed the hexagonal symmetry in all samples. Scanning electron microscope analysis of the crystals with the planar habit showed that the structure was actually a planar array of hexagonal filaments.

Attempts to grow crystals with $x < 0.2$ resulted in some crystals with the hexagonal phase and $x > 0.2$ (typically 0.22−0.24), and others with orthorhombic symmetry with $x < 0.10$, all within a given batch. Laue studies confirmed the orthorhombic structure of the low-x-value crystals, and showed evidence of a very large (~25Å) c axis dimension of the unit cell.

The Cs to W ratios were measured by x-ray fluorescence using Cs_2WO_4 as a standard, and are estimated to be accurate to at least 0.01 in x. The details of the analysis have been described previously.[2] Except for the low-x-value material, all samples were found within experimental error to have the nominal concentrations. The results of the x-ray fluorescence data on the samples used in this work are shown in Table I. No methods for oxygen determination were available; however, in this method of preparation we would expect the sample to be very near stoichometry.

Resistivity measurements were made by standard four-lead method using silver paint contacts with the sample mounted in a standard exchange gas system. The temperature was measured with a Ge thermometer for $T < 10$ K, a carbon-glass thermometer for $10 \leq T \leq 300$ K, and a copper-constantan thermocouple for $300 < T \leq 425$ K. Temperature stability and measurement accuracy were within ±0.02 K from 1.5 to 10 K and ±0.1 to 425 K. The error in the resistivity for a given sample is estimated to be about ±3%.

TABLE I. Results of x-ray fluorescence measurements for $0.16 \leq x_{nom} \leq 0.32$ Cs_xWO_3 samples. The sizeable concentration shifts at lower Cs concentrations are discussed in the text.

Batch No.	Nominal x	Measured x
1	0.32	0.31 ±0.01
2	0.30(a)	0.32 ±0.01
3	0.30(b)	0.30 ±0.01
4	0.28	0.28 ±0.01
5	0.27	0.33 ±0.01
6	0.26(a)	0.25 ±0.01
7	0.26(b)	0.27 ±0.01
8	0.24(a)	0.24 ±0.01
9	0.24(b)	0.25 ±0.02
10	0.22(a)	0.24 ±0.02
11	0.22(b)	0.24 ±0.01
12	0.20(a)	0.21 ±0.01
13	0.20(b)	0.21 ±0.01
14	0.18(a)	0.20 ±0.01
15	0.18(b)[a]	0.23 ±0.01
16	0.18(c)[a]	0.22 ±0.01
17	0.18(d)	0.23 ±0.01
18	0.16(a)[a]	0.23 ±0.01
19	0.16(b)[a]	0.22 ±0.01
20	0.16(c)	0.19 ±0.01
	Orthorhombic	0.06 ±0.01 to 0.10 ±0.01

[a]Also contained orthorhombic phase crystals.

Seebeck coefficient measurements were performed from 90 to 260 K at 10 K intervals. The filamentary samples were mounted between two isolated copper blocks, each with its own heater and copper-constantan thermocouple. The temperature gradient was set up across the crystal by offsetting the heater currents to produce ~3 K differential and any temperature-independent offset was taken into account by reversing the gradient. The coefficients were measured relative to copper, but since $|S_{Cu}| \leq 1.5$ μV while typical signals from Cs_xWO_3 were 20 μV, no corrections to obtain the absolute values were made.

Measurements of the chemical potential of single crystals of Cs_xWo_3 and Rb_xWO_3 were made using the configuration calomel−0.1N MCl−M_xWO_3, where M is Rb or Cs. This system is similar to that used previously for H_xWO_3.[4] A high-input impedance digital voltmeter was used for the potential measurements, and the system was allowed to come to equilibrium (≃10 min) before a measurement was taken. The cell emf's were referred to the H scale by subtracting the standard calomel emf of 0.242 V from the measured value.

The superconducting transition temperatures were mostly made by standard four-lead measurements with the current density kept below 10 A/cm^2 so that heating and flux flow effects were negligible and in all cases the current flow was parallel to the c axis. The transition temperature was taken to be the intercept on the temperature axis of the linear portion of the restored resistance curve. The value of T_c for several samples was measured by the ac susceptibility method using a self-inductance method at 80 kHz, and these measurements gave the same results as the dc resistivity method. The upper critical field, H_{c2}, was measured by sweeping the field from 0 to a maximum of 12.5 kG and recording the restored resistance as a function of H at different temperatures. The value of H_{c2} at each temperature was obtained by taking the intercept of the extrapolation of the linear portion R vs H curve on the H axis. Since all samples showed a 60° anisotropy in the plane perpendicular to the c axis and 180° anisotropy in the plane containing the c axis, measurements of H_{c2} vs T were generally made in the three directions corresponding to the maximum and minimum critical fields in the plane perpendicular to the c axis, and also along the c axis itself. Extrapolation of the H_{c2} vs T curves to $H_{c2}=0$ gave a check on the transition temperature.

III. RESULTS

The results of the x-ray fluorescence analysis of the samples used in this work are given in Table I. Except for nominal concentrations below $x=0.20$, the measured concentrations are close to the nominal concentrations. The sample batches labeled with a superscript a also contained some of the orthorhombic phase crystals, with $0.06 \leq x \leq 0.10$. In all cases the measured x values are used in reporting the data.

The resistivity, ρ, from $x=0.33$ down to $x=0.20$ were measured over the temperature range from 425 K down to the transition temperature T_c. In contrast to the Rb_xWO_3 in which a high-temperature anomaly occurs, the resistivity increases as a simple monotonic function over the entire temperature range for all x values. The resistivity at 250, 90, and 10 K as a function of x is shown in Fig. 2. The resistivity increases with decreasing x, with a distinct change in slope near $x=0.24$. Some resistivity measurements on the orthorhombic phase were made, and this material exhibited a large negative temperature coefficient, indicating either semiconducting or semimetal properties. A large, anisotropic magnetoresistance was also observed.

The Seebeck coefficient, S, measured as a function of T from 90 to 260 K shows a slow, approximately linear increase in magnitude with temperature at all concentrations, which is typical of most metals above 100 K. The variation of S with x is shown at four

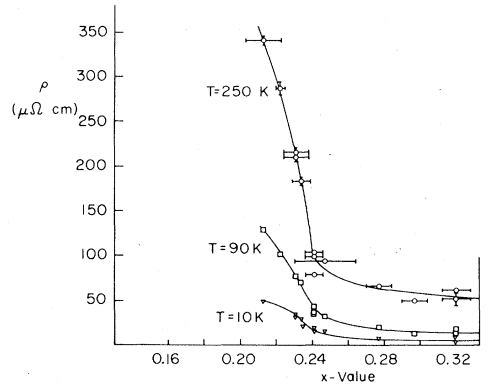

FIG. 2. Resistivity as a function of x value for Cs_xWO_3, plotted at three temperatures. The scaling of ρ with x, and the inflection in ρ near $x=0.24$, are discussed in the text. The solid lines are for the purpose of a visual aid only.

temperatures in Fig. 3. The increase in the magnitude of S with decreasing x indicates a decrease in the number of carriers with decreasing Cs concentration and qualitatively supports the idea that the metal ion contributes about one electron to the conduction band. Furthermore, the magnitudes of S are 5 to 10 times larger than those found in most metals, which probably reflects the relatively low number of charge carriers in these materials.

The chemical potential of a number of samples is plotted as a function of x value for both Cs_xWO_3 and Rb_xWO_3 in Fig. 4. Each point on the plot represents a different sample, and while there is considerable scatter in the data, the trend suggests a minimum near $x=0.24$, which could result if some type of

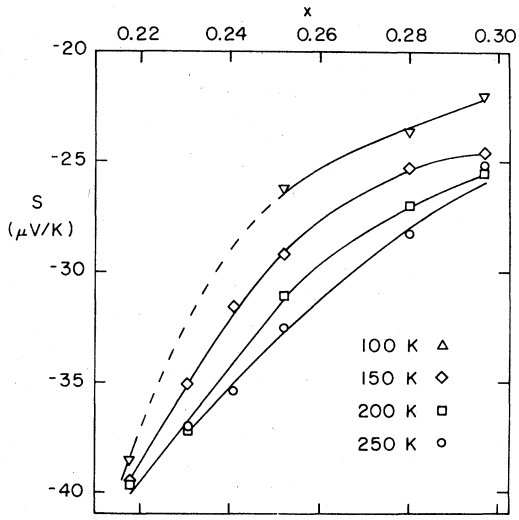

FIG. 3. Seebeck coefficient as a function of x value for Cs_xWO_3, plotted at four temperatures. The change in S with changing Cs content can be explained in terms of the changing charge carrier concentration.

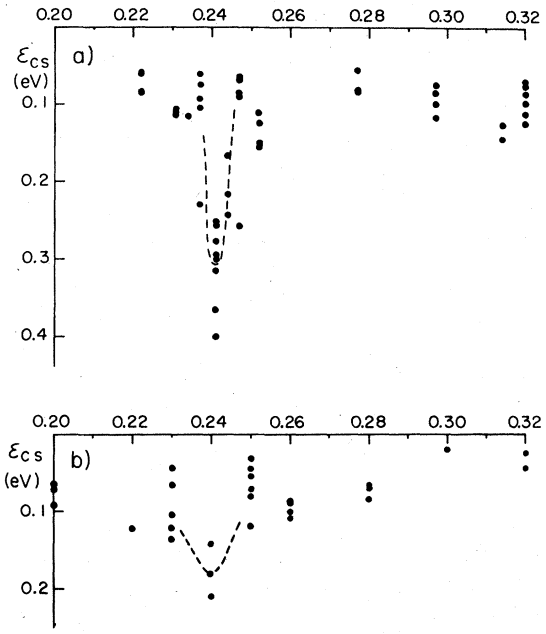

FIG. 4. Chemical-potential ϵ_{cs} results as a function of x value: (a) Cs_xWO_3; (b) Rb_xWO_3. The behavior near $x=0.24$ is discussed in the text.

structural change occurs near this concentration.

The superconducting transition temperature of Cs_xWO_3 for $0.19 \leq x \leq 0.33$ is shown in Fig. 5. Since in all cases the same transition temperature was obtained by both resistivity and ac susceptibility methods, no distinction is made in the measurement method in the data shown in Fig. 5. At $x=0.19$, $T_c \simeq 6.7$ K and drops slowly with increasing x to a T_c of about 6 K at $x=0.23$. Above $x=0.23$ T_c decreases more rapidly with concentration to $T_c=4$ K at $x=0.25$, above which a more gradual, nearly linear, decrease with x is observed up to $x=0.30$ where $T_c=2$ K. The samples for $x>0.30$ showed no transition down to 1.4 K, the limit of our system, but the data of Bevolo[5] and Sweedler[6] are shown. There has been good agreement for T_c obtained in different laboratories for $x=0.33$. The transition widths were about 0.05 K from the ac measurements, and 0.05 to 0.1 K from resistivity measurements. The fact that the resistivity transitions were slightly wider was assumed to be due to the finite current flow. The fractional volume of the sample which was superconducting as measured in ac susceptibility studies ranged from 70 to 95%. The lower values occurred in the larger samples (~ 1 mm) and probably reflected a skin-depth effect. The slightly broader transition widths observed by the susceptibility method in a few samples may be due to small surface effects. It should be kept in mind the susceptibility was measured at a considerably higher frequency (~ 80 MHz) than is normally used (~ 30 Hz).

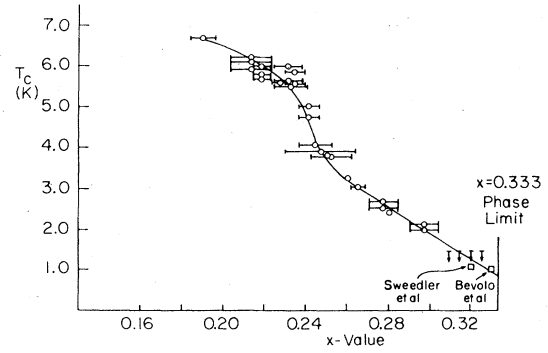

FIG. 5. Transition temperature as a function of x value for $0.19 \leq x \leq 0.33$ Cs_xWO_3 samples. The change in T_c with x and the sharper enhancement near $x=0.24$ are discussed in the text.

The variation of the upper critical field H_{c2} with the angle of the applied field (the angles are defined in Fig. 1.) for $Cs_{0.20}WO_3$ is shown in Fig. 6. This behavior is qualitatively reproduced for all concentrations measured. There was considerable scatter in the magnitude of H_{c2} at $t(=T/T_c)=0.8$ for different

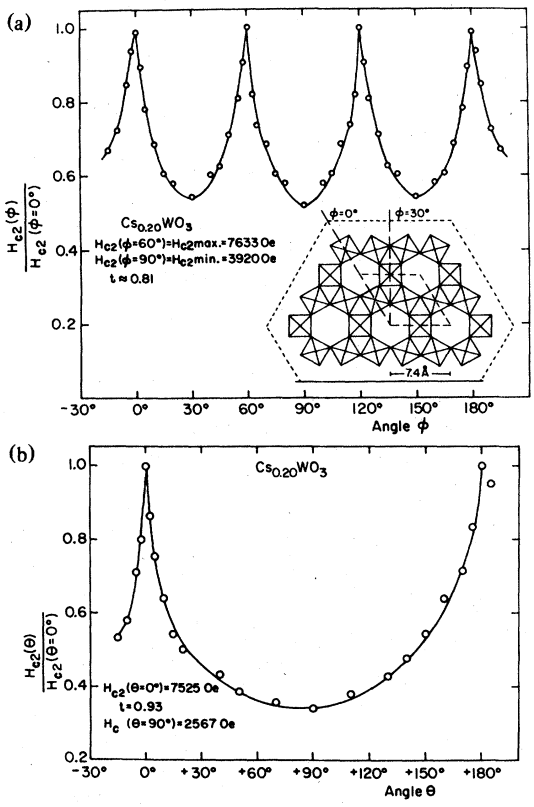

FIG. 6. Typical anisotropy data for $Cs_{0.20}WO_3$: (a) basal plane (ϕ rotation); (b) azimuthal (θ rotation). This behavior is quite typical of that observed in all Cs_xWO_3 samples tested.

samples of a given x value. This may be due to a contribution from surface pinning or H_{c3} effects. Another possible explanation of the large fluctuation in the H_{c2} values is that H_{c2} is dependent on ρ while T_c is not, so that fluctions in ρ could produce such a result. Unfortunately this possibility would be very difficult if not impossible to check since it would require mounting and demounting several fragile samples. Due to the large scatter, one can only state that the *trend* of the data is that H_{c2} scales with T_c. The 60° anisotrophy parameter, as defined by the relation $\alpha=(H_{c2}^{\max}-H_{c2}^{\min})/H_{c2}^{\text{av}}$ in the plane perpendicular to the c axis, is temperature independent down to a reduced temperature of 0.4, but shows a large variation (1.28 to 0.4) among different samples which appears to be uncorrelated with x. The values of H_{c2} at $t=0.8$ and α were quite consistent at $x=0.30$ for all batches, with values of 50 G at $\phi=0°$, 110 G at $\phi=30°$, and $\alpha=1.28$. The low values of H_{c2} near $x=0.33$ may be indicative that the behavior approaches that of type-I materials, as suggested previously by Bevolo.[5]

IV. DISCUSSION

The data presented here show that the dramatic behavior of the transport properties with x value and temperature observed in Rb_xWO_3 are not present in Cs_xWO_3, although the data does indicate that possibly some vestiges of the drastic change in behavior observed near $n=0.25$ in Rb_xWO_3 are observed in Cs_xWO_3 near this same concentration. However, the results for Cs_xWO_3, with the exception of the H_{c2} data, were in general more reproducible between crystal batches and the properties less sensitive to the growth parameters than for Rb_xWO_3, especially in the range $0.26\leq x\leq 0.33$, indicating a somewhat more stable structure in Cs_xWO_3. It thus seems reasonable to attempt to describe the responsible mechanisms in somewhat more detail than was done for Rb_xWO_3.[2]

The resistivity data, as shown in Fig. 2, shows an overall trend of decreasing ρ with increasing x which is consistent with an increasing number of charge carriers, and, perhaps also, a reduced number of channel site vacancies to act as scatterers. The inflection in the ρ vs T plot at $x=0.24$ in Fig. 2 is in contrast to the behavior of ρ in Rb_xWO_3. In Rb_xWO_3 the ρ_{4K} and ρ_{300K} follow within experimental error the Nordheim relation[7] for simple alloys, i.e., $\rho\propto x(0.33-x)$. The inflection in ρ at $x=0.24$ and the possible anomaly in the chemical potential near this same concentration show more evidence for an anomolous behavior in Cs_xWO_3 near $x=0.24$–0.25 than the corresponding parameters in Rb_xWO_3. As will be discussed below, all the other parameters (ρ vs T, Seebeck coefficients, Hall coefficients, and T_c) give a strong indication of some type of phase transition near $x=0.25$ in Rb_xWO_3, but a much weaker, or no indication of such a transition in Cs_xWO_3. The inflection in the ρ vs x plot with increasing x for Cs_xWO_3 is not easily understood. A loss of stability in the lattice with decreasing x value could result in an increase in the electron-phonon interaction and consequently a more rapid increase in ρ vs T than would be expected just from a decrease in carriers or an increase in scatterers.

The Seebeck coefficient, shows a small, nearly linear increase in magnitude with increasing temperature. The variation of S with x, shown in Fig. 3 at several temperatures, is typical of behavior in electron diffusion limited systems, and qualitatively obeys the free-electron prediction, $S\propto x^{-2/3}$. In contrast to the Rb_xWO_3 data, there is no evidence in these data which would indicate unusual behavior either as a function of temperature or Cs concentration. As stated before, the data indicate that there is a smooth decrease in the number of conduction electrons with decreasing x.

While there is considerable scatter in the emf, ϵ_{cs}, of the chemical potential cell as plotted vs x in Fig. 4, there appears to be a minimum near $x=0.24$ for both Cs_xWO_3 and Rb_xWO_3. The interpretation of these data is difficult since there are a number of parameters on which the chemical potential depends[8] and which would be x dependent, e.g., reduction of W^{6+} to W^{5+} (which would be linear in x), changes in the energy at the Fermi surface, a change in the free energy of distributing x moles of the metal in one mole of WO_3, etc. It does, however, provide some indication of a change in behavior of both materials near $x=0.24$.

The variation of T_c with x, as shown in Fig. 5, indicates an inflection point near $x=0.24$, which may be indicative of some change in the superconducting mechanism, or possibly a phase transition at this composition. However, the behavior is far less striking than that observed in Rb_xWO_3, giving rather weak evidence for any phase transition in the Cs_xWO_3 as is believed to occur in Rb_xWO_3.

Since the necessary parameters are known or may be estimated, one can calculate some possibly useful parameters from McMillan's[9] theory for superconductors in the dirty limit. This calculation could not be carried out for Rb_xWO_3 because of the peculiar behavior of the heat capacity at low temperatures.[5] The resistivity of Cs_xWO_3 is such that the dirty limit should certainly be satisfied. The expression for McMillan's λ is

$$\lambda=\frac{1.04+\mu^*\ln(\Theta_D/1.45T_c)}{(1-0.62\mu^*)\ln(\Theta_D/1.45T_c)-1.04},$$

where Θ_D is the Debye temperature and μ^* is the Coulomb pseudopotential. Bevolo *et al.*[5] find $\Theta_D=380$ K for $Cs_{0.33}WO_3$, and nearly the same value for monoclinic WO_3, which might be considered the

unfilled structure. Thus, a reasonable assumption is that Θ_D is independent of x value. This does not preclude the possibility that changes in the phonon spectrum are a major contribution to the behavior of T_c with x. The electron-phonon coupling responsible for the superconductivity could involve only a few modes which could change drastically while producing only small changes in Θ_D. Wolfram[10] has shown for the overlapping tungsten t_{2g} d orbitals and the oxygen $p\pi$ orbitals which form the conduction band of M_xWO_3 that the density of states, $\rho(E_F)$, should be linear in x and this dependence has been observed by Shanks for Na_xWO_3.[11] Ngai and Silberglitt[12] have theoretically predicted the relation $\mu^* = 0.15x$. While this result is based on results in the cubic or tetragonal phase, it depends only on the WO_6 octahedra, and thus should be essentially structure independent. Using these parameters, the values of λ vs x were calculated and are given in Table II. The value of λ is relatively small, typical of a weakly coupled superconductor, and decreases with increasing x. The values of McMillan's "band-structure" density of states $N_{bs}(0)$ can be calculated from the relation

$$N_{bs}(a) = 3\gamma(x)/2\pi^2 k_B(1+\lambda),$$

where k_B is Boltzman's constant and $\gamma(x)$ is the electronic specific heat. Taking ρ (E_F) and thus γ linear in x and using the values $\gamma(0.33) = 2.15$ and $\gamma(0.00) = 0.6$ mJ/mole K^2 (pure WO_3) as measured by Bevolo *et al.*,[5] the resulting electronic specific heat is given by

$$\gamma(x) = 0.6 + 1.55(x/0.33) \quad .$$

TABLE II. McMillan parameter λ and $N_{bs}(0)$ calculated for the different measured Cs concentrations, x. The values of T_c are the measured values and the values of γ were obtained from γ for $Cs_{0.33}WO_3$ and WO_3 assuming a linear relation between γ and x.

x	T_c (K)	λ calculated	γ $\left(\frac{\text{mJ}}{\text{mole K}^2}\right)$	$[N_{bs}(0)]_{\text{calculated}}$ $\left(\frac{\text{No. States}}{\text{eV Formula-unit}}\right)$
0.19	6.7	0.45	1.49	0.22
0.20	6.2	0.44	1.54	0.23
0.21	6.0	0.44	1.59	0.24
0.23	5.8	0.44	1.68	0.25
0.24	5.0	0.42	1.73	0.26
0.25	3.8	0.39	1.77	0.27
0.26	3.3	0.39	1.82	0.28
0.28	2.5	0.35	1.92	0.30
0.30	2.0	0.34	2.01	0.32
0.33	1.1[a]	0.31	2.15	0.35

[a]Data from Sweedler *et al.* (Ref. 19) and Bevolo *et al.* (Ref. 20).

The experimental value of Bevolo for γ at $x = 0$ was used, although pure WO_3 is an insulator and γ should be 0. If γ is taken to be 0, for WO_3, the calculated parameters are changed slightly, but the trend is the same. If a phase transition does occur near $x = 0.24$, the assumed linear relation between γ and x may not be valid. The results of the calculation of $N_{bs}(0)$ using this dependence are also given in Table II. The linearity of $N_{bs}(0)$ with x is, of course, as expected for this model, while in contrast to the usual situation, γ increases with a decreasing density of states in Cs_xWO_3.

In the theoretical definition $\gamma = N(0)\langle I^2\rangle/M\langle\omega^2\rangle$ where $\langle I^2\rangle$ is the mean-square average of the electron-phonon matrix element over the Fermi surface, M is the atomic mass and $\langle\omega^2\rangle$ is the mean-squared-average phonon frequency, McMillan has argued that the product $N(0)\langle I^2\rangle$ is roughly constant for a given class of materials, and that changes in λ (and T_c) come from the lattice related product $M\langle\omega^2\rangle$. Since then Weber[13] has contended $M\langle\omega^2\rangle$ remains roughly constant while $N(0)\langle I^2\rangle$ governs changes in λ while more recently Varma and Dynes[14] have suggested both $N(0)\langle I^2\rangle$ and $\langle I^2\rangle/M\langle\omega^2\rangle$ are approximately constant for materials of similar lattice and electronic structure leaving λ only dependent on $N(0)$. This latter suggestion cannot be true for the Cs_xWO_3 or Rb_xWO_3 since γ (and T_c) increases with decreasing x and consequently decreasing $N(0)$. The idea that $M\langle\omega^2\rangle$ is roughly constant would require $\langle I^2\rangle$ to increase rapidly to overcome the decrease in $N(0)$ as x decreases, which would mean an increased electron-phonon interaction with little or no change in lattice stiffness, which seems improbable. Thus, for Cs_xWO_3, McMillan's original idea seems more likely. Here, $\langle I^2\rangle$ must also increase as $N(0)$ decreases, but not as rapidly as for the other two suggestions, since $M\langle\omega^2\rangle$ can also vary. It would appear from the T_c data, and also the resistivity data that both $1/M\langle\omega^2\rangle$ and $\langle I^2\rangle$ are somehow enhanced with increased insertion ion vacancies in Cs_xWO_3.

While the scatter in the raw data for H_{c2} precludes any quantitative analysis, several general conclusions can be drawn. The hexagonal, 60°, anisotropy in the plane perpendicular to the c axis and 180° anisotropy in the plane containing the c axis has been observed in all samples of the tungsten bronzes we have measured. Furthermore, the trend of all the data is that the critical fields, at fixed $t(=T/T_c)$, decrease with increasing concentrations from several kilogauss at the low x values down to about 100 G as x approaches $x = 0.33$ in both Cs_xWO_3 and Rb_xWO_3. To compare the data to the Maki[15] theory of H_{c2} for dirty Type-II superconductors with a spherical Fermi surface, the relation

$$H_{c2}(0) = -(T_c)\left(\frac{dH_{c2}}{dT}\right)_{T_c} \Big/ 1.4635$$

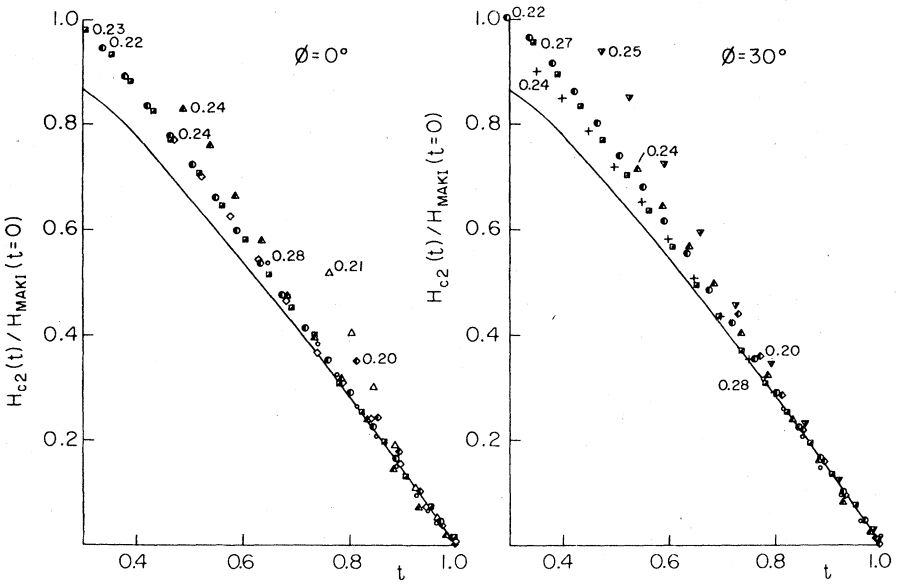

FIG. 7. Reduced upper critical field as a function of reduced temperature for the two unique basal-plane orientations. The solid curve and the values of H_{c2} $(t=0)$ used to normalize the data were calculated from the Maki theory for dirty superconductors (Ref. 13).

was used to calculate H_{c2} (0). The ratio $H_{c2}(t)/H_{c2}(0)$ is plotted as a function of reduced temperatue for $\phi=30°$ and $\phi=60°$ in Fig. 7. All concentrations give essentially the same dependence on reduced temperature. The solid curve is calculated from the relation given by Maki[15]

$$\ln t + f_o\left[\frac{0.87}{2\pi t}\frac{H_{c2}(t)}{H_{c2}(0)}\right]=0\ ,$$

where $f_o(\xi)=\mathrm{Re}[\Psi(\frac{1}{2}+\xi)-\Psi(\frac{1}{2})]$ and Ψ is the digamma function. The calculated curve in all cases falls below the data, which is consistent with the qualitative prediction of Hohenberg and Werthamer[16] that H_{c2} for a spherical Fermi surface will always fall below the value for an anisotropic Fermi surface. It should be pointed out that the anisotropy ratio of the critical field, as defined in Sec. III, is essentially temperature independent.

No current general theory predicts a 60° anisotropy in H_{c2}, for hexagonal structures, and in fact such a symmetry is of course not allowed in the effective-mass theories where the effective mass is treated as a second rank tensor. Entel and Peter[17] and Entel [18] have performed calculations on measurements of 60° anisotropy of $Cs_{0.1}WO_{2.9}F_{0.1}$ made earlier in this laboratory.[19] The experimental results were described by a mixture of contributions from two uncorrelated bands, i.e., no electron-phonon coupling between the bands. Both the Cs and F atoms were treated as impurities. In order to explain the anisotropy in H_{c2} in $Cs_{0.1}WO_{2.9}F_{0.1}$, it was necessary to assume very flat bands and a high density of states. It should be possible to extend this theory to the "pure" tungsten bronzes, but apparently no such extension has yet been made.

V. SUMMARY

The most interesting aspect of the data on Cs_xWO_3 is the fact that the phase transitions, both the one with temperature and the one with composition, observed in Rb_xWO_3 are absent or strongly suppressed. The temperature-dependent transition appears to be totally absent, and while there is some indication of a possible phase change with x near $x=0.24$ in the resistivity, transition temperature, and possibly the chemical potential, the effects of such a phase change, if one exists, are greatly reduced in the Cs_xWO_3 system. All previous data indicate that the band structure in the hexagonal tungsten bronzes is approximately independent of the metal ion-type and each metal ion contributes its electron to the tungsten conduction band. This would seem to indicate that the major difference between the behavior of Rb_xWO_3 and Cs_xWO_3 is due to differences in the lattice properties. This can perhaps be understood from the fact that the radius of the channel site in hexagonal M_xWO_3 is about 1.63 Å and the Rb and Cs ionic radii are 1.47 and 1.69 Å, respectively. Thus the Rb ion is relatively free to move about in the channel site while the Cs ions are much more rigid. The x-ray studies indicate that with increasing x value the unit cell for potassium $(r=1.33)$ contracts, that it remains essentially constant for rubidium, and ex-

pands for cesium. It would seem that the Cs_xWO_3 is a more tightly bound system than the Rb_xWO_3, thus giving it a more stable structure and suppressing the phase changes. More work is obviously necessary to understand the interesting behavior of these materials, particularly studies of the phonon spectra, higher precision studies of possible structural transformations, and investigations which will yield more information about the band structure and how it may change with metal ion-type, concentration, and temperature.

ACKNOWLEDGMENTS

We acknowledge the assistance of L. Pierce in the preparation of crystals. This work was supported by NSF Grants No. DMR 76-10845 and No. DMR 78-21612.

*Present address: Naval Res. Lab, Code 5285, Wash., D. C. 20375.

[1]P. Hagenmuller, in *Comprehensive Inorganic Chemistry,* (Pergammon, New York, 1973), Vol. 4, p. 541; P. G. Dickens, and M. S. Whittingham, Q. Rev. Chem. Soc. 22, 30 (1968).

[2]R. K. Stanley, R. C. Morris, and W. G. Moulton, Phys. Rev. B 20, 1903 (1979).

[3]J. B. Goodenough, Bull. Soc. Chim. Fr. 4, 1200 (1965); A. Ferretti, D. B. Rogers, and J. B. Goodenough, J. Phys. Chem. Solids 26, 2007 (1965).

[4]R. S. Crandall, P. J. Wojtowicz, and B. W. Faughnen, Solid State Commun. 18, 1409 (1976).

[5]A. O. Bevolo, H. R. Shanks, P. H. Sidles, and G. C. Danielson, Phys. Rev. B 9, 3220 (1974).

[6]A. R. Sweedler, C. J. Raub, and B. T. Matthias, Phys. Lett. 18, 108 (1965).

[7]J. M. Ziman, *Electrons and Phonons* (Oxford University, New York, 1960), p. 267–268.

[8]R. S. Crandall and B. W. Faughnen, Phys. Rev. B 16, 1750 (1977).

[9]W. L. McMillan, Phys. Rev. 167, 331 (1968).

[10]T. Wolfram, Phys. Rev. Lett. 29, 1383 (1972).

[11]H. R. Shanks, Solid State Commun. 15, 753 (1974).

[12]K. L. Ngai and R. Silberglitt, Phys. Rev. B 13, 1032(1976).

[13]W. Weber, Phys. Rev. B 8, 5093 (1973).

[14]C. M. Varma and R. C. Dynes, in *Superconductivity in d- and f-Band Metals,* edited by D. H. Douglass (Plenum, New York, 1976), p. 507.

[15]K. Maki, Phys. Rev. 148, 362 (1966).

[16]P. C. Hohenberg and N. R. Werthamer, Phys. Rev. 153, 493 (1967).

[17]P. Entel and M. Peter, in *Anisotropy Effects in Superconductors,* edited by H. W. Weber (Plenum, New York, 1976), p. 47.

[18]P. Entel, Solid State Commun. 19, 1233 (1976).

[19]M. R. Skokan, R. C. Morris, and W. G. Moulton, Phys. Rev. B 13, 1077 (1976).